

Realization of a Knill-Laflamme-Milburn controlled-NOT photonic quantum circuit combining effective optical nonlinearities

Ryo Okamoto^{a,b}, Jeremy L. O'Brien^c, Holger F. Hofmann^d, and Shigeki Takeuchi^{a,b,1}

^aResearch Institute for Electronic Science, Hokkaido University, Sapporo 060-0812, Japan; ^bThe Institute of Scientific and Industrial Research, Osaka University, 8-1 Mihogaoka, Ibaraki, Osaka 567-0047, Japan; ^cCenter for Quantum Photonics, H. H. Wills Physics Laboratory and Department of Electrical and Electronic Engineering, University of Bristol, Merchant Venturers Building, Woodland Road, Bristol BS8 1UB, United Kingdom; and ^dGraduate School of Advanced Sciences of Matter, Hiroshima University, Hiroshima 739-8530, Japan

Edited by Alain Aspect, Institut d'Optique, Orsay, France, and approved May 5, 2011 (received for review December 21, 2010)

Quantum information science addresses how uniquely quantum mechanical phenomena such as superposition and entanglement can enhance communication, information processing, and precision measurement. Photons are appealing for their low-noise, light-speed transmission and ease of manipulation using conventional optical components. However, the lack of highly efficient optical Kerr nonlinearities at the single photon level was a major obstacle. In a breakthrough, Knill, Laflamme, and Milburn (KLM) showed that such an efficient nonlinearity can be achieved using only linear optical elements, auxiliary photons, and measurement [Knill E, Laflamme R, Milburn GJ (2001) *Nature* 409:46–52]. KLM proposed a heralded controlled-NOT (CNOT) gate for scalable quantum computation using a photonic quantum circuit to combine two such nonlinear elements. Here we experimentally demonstrate a KLM CNOT gate. We developed a stable architecture to realize the required four-photon network of nested multiple interferometers based on a displaced-Sagnac interferometer and several partially polarizing beamsplitters. This result confirms the first step in the original KLM “recipe” for all-optical quantum computation, and should be useful for on-demand entanglement generation and purification. Optical quantum circuits combining giant optical nonlinearities may find wide applications in quantum information processing, communication, and sensing.

nonlinear optics | quantum optics | linear optics | quantum gates

Several physical systems are being pursued for quantum computing (1)—promising candidates include trapped ions, neutral atoms, nuclear spins, quantum dots, superconducting systems, and photons—while photons are indispensable for quantum communication (2, 3) and are particularly promising for quantum metrology (4, 5). In addition to low-noise quantum systems (typically two-level “qubits”) quantum information protocols require a means to interact qubits to generate entanglement. The canonical example is the controlled-NOT (CNOT) gate, which flips the state of the polarization of the “target” photon conditional on the “control” photon being horizontally polarized (the logical “1” state). The gate is capable of generating maximally entangled two-qubit states, which together with one-qubit rotations provide a universal set of logic gates for quantum computation.

The low-noise properties of single photon qubits are a result of their negligible interaction with the environment, however, the fact that they do not readily interact with one-another is problematic for the realization of a CNOT or other entangling interaction. Consequently it was widely believed that matter systems, such as an atom or atom-like system (6), or an ensemble of such systems (7), would be required to realize such efficient optical nonlinearities. Indeed the first proposals for using linear optics to benchmark quantum algorithms require exponentially large physical resources (8–10).

In 2001, KLM made the surprising discovery that a scalable quantum computer could be built from only linear optical networks, and single photon sources and detectors (11). In fact, it was even surprising to KLM themselves, as they had initially intended to prove the opposite. The KLM recipe consists of two parts: an optical circuit for a CNOT gate using linear optics, single photon sources (12), and photon number-resolving detectors (13); and a scheme (14, 15) for increasing the success probability of this CNOT gate ($P = 1/16$) arbitrarily close to unity, where the probabilistic CNOT gates generate the entangled states used as a resource for the implementation of controlled unitary operation based on quantum teleportation (16, 17). This discovery opened the door to linear optics quantum computation and has spurred world-wide theoretical and experimental efforts to realize such devices (18), as well as new quantum communication schemes (2) and optical quantum metrology (5). Inspired by the KLM approach, a number of quantum logic gates using heralded photons and event postselection have been proposed and demonstrated (19–28). Furthermore, optical quantum circuits combining these gates have been demonstrated (29–33). In this context, photonic quantum information processing using linear optics and postselection is one of the promising candidates in the quest for practical quantum information processing (18).

Knill-Laflamme-Milburn C-NOT Gate

Interestingly, none of these gates realized so far (19–28) actually used the original KLM proposal of a simple measurement-induced nonlinearity: either the gates are not heralded (the resultant output photons themselves have to be measured and destroyed) or rely on additional entanglement effects; as we explain below, the KLM scheme is based on a direct implementation of the nonlinear sign-shift (NS) gate that relies on the interaction with a single auxiliary photon at a beam splitter (BS). The NS gate is thus based on the efficient optical nonlinearity induced by single photon sources and detectors. While a measurement-induced nonlinearity has been verified by a conditional phase shift for one specific input (21), the complete function of a NS gate for arbitrary inputs has not been demonstrated. Moreover, it is an important remaining challenge to combine the nonlinearities into a network such as the KLM-CNOT gate, because this requires a more reliable control of optical coherence than a nonlinearity acting on a single beam, especially because nonlinearities tend to couple modes to produce additional and often unexpected noise patterns. Specifically, it is a difficult task to implement the nested interferometers needed to perform the multiple classical

Author contributions: R.O., J.L.O'B., H.F.H., and S.T. designed research; performed research; contributed new reagents/analytic tools; analyzed data; and wrote the paper.

The authors declare no conflict of interest.

This article is a PNAS Direct Submission.

Freely available online through the PNAS open access option.

¹To whom correspondence should be addressed. E-mail: takeuchi@es.hokudai.ac.jp.

and quantum interferences that form the elements of the quantum gate operation, which has prevented the realization of the KLM-CNOT gate.

The key element in the KLM CNOT gate is the nondeterministic NS gate (Fig. 1A), which operates as follows: When a superposition of the vacuum state $|0\rangle$, one photon state $|1\rangle$ and two-photon state $|2\rangle$ is input into the NS gate, the gate flips the sign (or phase) of the probability amplitude of the $|2\rangle$ component: $|\psi\rangle = \alpha|0\rangle + \beta|1\rangle + \gamma|2\rangle \rightarrow |\psi'\rangle = \alpha|0\rangle + \beta|1\rangle - \gamma|2\rangle$. Note that this operation is nondeterministic—it succeeds with probability of $P = 1/4$ —however, the gate always gives a signal (photon detection) when the operation is successful.

The Nonlinear Sign-Shift Gate

A CNOT gate can be constructed from two NS gates as shown schematically in Fig. 2A (11). Here the control and target qubits are encoded in optical mode or path (“dual-rail encoding”), with a photon in the top mode representing a logical 0 and in the bottom a logical 1. The target modes are combined at a 1/2 reflectivity BS (BS3), interact with the control 1 mode via the central Mach-Zehnder interferometer (MZ), and are combined again at a 1/2 reflectivity BS (BS4) to form another MZ with the two target modes, whose relative phase is balanced such that, in the absence of a control photon, the output state of the target photon is the same as the input state. The goal is to impart a π phase shift in the upper path of the target MZ, conditional on the control photon being in the 1 state such that the NOT operation will be implemented on the target qubit. When the control input is 1, quantum interference (34) between the control and target

photons occurs at BS1: $|1\rangle_{C_1}|1\rangle_{T_0} \rightarrow |2\rangle_{C_1}|0\rangle_{T_0} - |0\rangle_{C_1}|2\rangle_{T_0}$. In this case the NS gates each impart a π phase shift to these two-photon components: $|2\rangle_{C_1/T_0} \rightarrow -|2\rangle_{C_1/T_0}$. At BS2 the reverse quantum interference process occurs, separating the photons into the C_1 and T_0 modes, while preserving the phase shift that was implemented by the NS gates. In this way the required π phase shift is applied to the upper path of the target MZ, and so CNOT operation is realized.

An NS gate can be realized using an optical circuit consisting of three beam splitters, one auxiliary single photon, and two-photon number-resolving detectors (Fig. 1B) (11). The NS gate is successful, i.e., $|\psi\rangle \rightarrow |\psi'\rangle$, when one photon is detected at the upper detector and no photons at the lower detector. This outcome

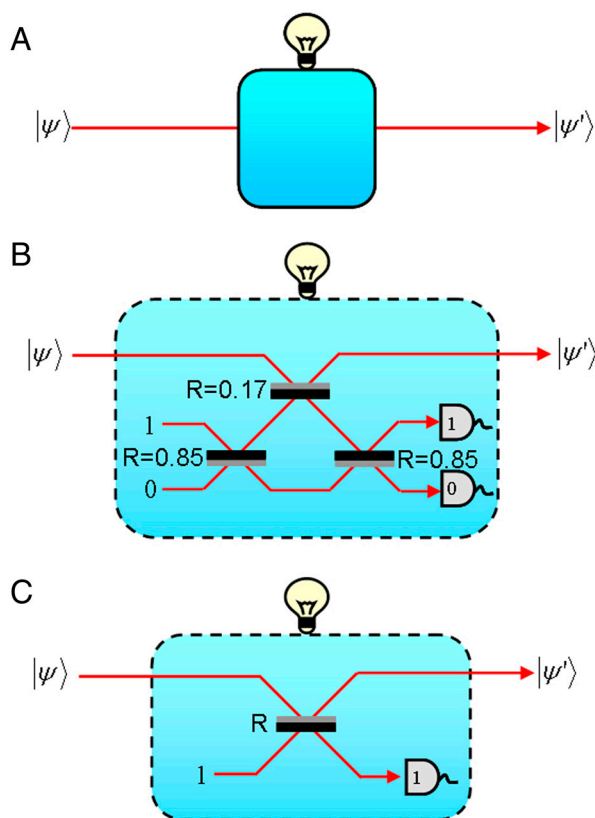


Fig. 1. The KLM NS gate. (A) If the NS gate succeeds it is heralded; indicated conceptually by the light globe. (B) The original KLM NS gate is heralded by detection of a photon at the upper detector and no photon at the lower detector. Gray indicates the surface of the BS from which a sign change occurs upon reflection. (C) A simplified KLM NS gate for which the heralding signal is detection of one photon.

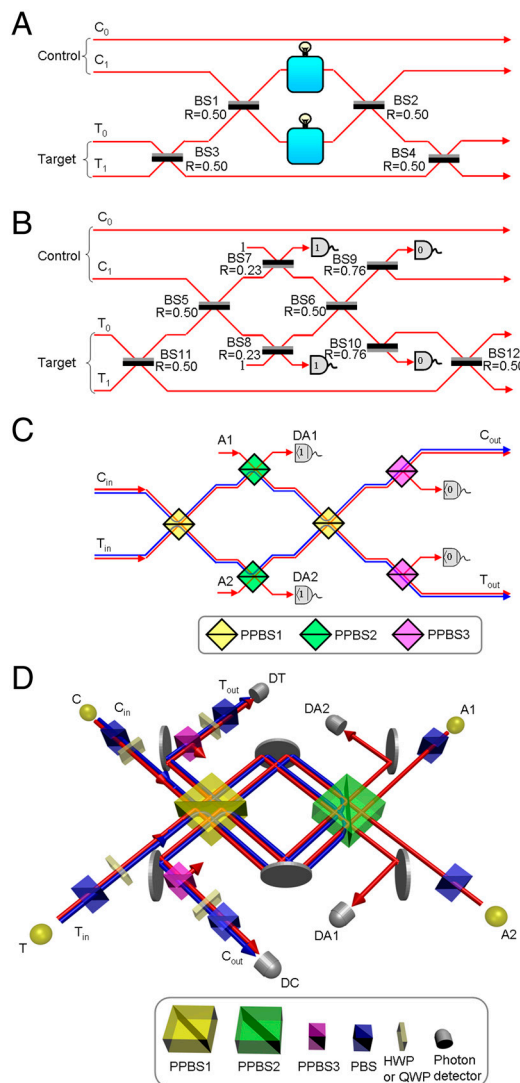


Fig. 2. The KLM CNOT gate. (A) The gate is constructed of two NS gates; the output is accepted only if the correct heralding signal is observed for each NS gate. Gray indicates the surface of the BS from which a sign change occurs upon reflection. (B) The KLM CNOT gate with simplified NS gate. (C) The same circuit as (B) but using polarization encoding and PPBSs. (D) The stable optical quantum circuit used here to implement the KLM CNOT gate using PPBSs and a displaced-Sagnac architecture. The target MZ, formed by BS11 and BS12 in Fig. 2B, can be conveniently incorporated into the state preparation and measurement, corresponding to a change of basis, as described in the caption to Fig. 3. The blue line indicates optical paths for vertically polarized components, and the red line indicates optical paths for horizontally polarized components.

when the C qubit is 1. The (classical) fidelity of this process $F_{ZZ \rightarrow ZZ}$, defined as the ratio of transmitted photon pairs in the correct output state to the total number of transmitted photon pairs, is 0.87 ± 0.01 .

Because almost all the errors conserve horizontal/vertical polarization, the process fidelity F_P of the quantum coherent gate operation can be determined from the fidelities obtained from only three sets of orthogonal input- and output states (see *Appendix: Derivation of the Process Fidelity*),

$$F_P = (F_{ZZ \rightarrow ZZ} + F_{XX \rightarrow XX} + F_{XZ \rightarrow YY} - 1)/2. \quad [1]$$

The measurement result of the input-output probabilities in the XX basis are shown in Fig. 3B, where the basis states are $\{|0_X\rangle \equiv 1/\sqrt{2}(|0\rangle + |1\rangle), |1_X\rangle \equiv 1/\sqrt{2}(|0\rangle - |1\rangle)\}$; the fidelity is $F_{XX \rightarrow XX} = 0.88 \pm 0.02$. To obtain $F_{XZ \rightarrow YY}$, we detected the YY basis output from XZ basis inputs, as shown in Fig. 3C. The Y basis states are $\{|0_Y\rangle \equiv 1/\sqrt{2}(|0\rangle + i|1\rangle), |1_Y\rangle \equiv 1/\sqrt{2}(|0\rangle - i|1\rangle)\}$. The fidelity is $F_{XZ \rightarrow YY} = 0.81 \pm 0.02$. Using Eq. 1, we find a process fidelity of $F_P = 0.78$.

A more intuitive measure of how all other possible gate operations (input and output states) perform is given by the average gate fidelity \bar{F} , which is defined as the fidelity of the output state averaged over all possible input states. This measure of the gate performance is related to the process fidelity by (36, 37)

$$\bar{F} = (dF_P + 1)/(d + 1), \quad [2]$$

where d is the dimension of the Hilbert space ($d = 4$ for a 2 qubit gate). Based on Eqs. 1 and 2, our results show that the average gate fidelity of our experimental quantum CNOT gate is $F = 0.82 \pm 0.01$.

Discussion

The data presented above confirm the realization of the CNOT gate proposed by KLM, which is an optical circuit combining a pair of efficient nonlinear elements induced by measurement. This result confirms the first step in the KLM recipe for all-optical quantum computation and illustrates how efficient nonlinearities induced by measurement can be utilized for quantum information science; such measurement-induced optical nonlinearities could also be an alternative to nonlinear media used for quantum nondemolition detectors (39) or photonic pulse shaping (40). By emulating fundamental nonlinear processes, such measurement-induced optical nonlinearities can also improve our understanding of the quantum dynamics in nonlinear media. Conversely, future technical progress may permit the replacement of these effective optical nonlinearities in the network by approaches based on nonlinearities in material systems such as atoms (6), solid state devices (41), hybrid systems (42), or optical fiber Kerr nonlinearities (43). In this context, our demonstration provides an experimental test for quantum networks based on nonlinear optical elements and may serve as a reference point for comparisons with future networks using other optical nonlinearities. In particular, the present results may be useful as a starting point for a more general analysis of quantum error propagation in nonlinear optical networks. Our device will be useful for conventional and cluster state approaches to quantum computing (38), as well as quantum communication (2), and optical quantum metrology (5). This circuit could be implemented using an integrated waveguide architecture (28), in which case a dual-rail encoding could conveniently be used.

In the present tests of the performance of CNOT gate operation, we used threshold detectors to monitor the output state. For applications in which the output state cannot be monitored, high-efficiency number-resolving photon detectors (13) could be used at DA1 and DA2 to generate the heralding signals. We also used spontaneous parametric fluorescence as single photon sources.

Note that alternative approaches that do not follow the KLM recipe as closely can be useful for scalable linear optics quantum information processing (18). For all these approaches, further progress in on-demand single photon sources and practical photon resolving detectors will be crucial to ensure reliable operation.

Appendix: Derivation of the Process Fidelity

The PPBSs used to realize the KLM CNOT gate preserve the horizontal/vertical polarization with high fidelity. In the quantum CNOT operation, these polarizations correspond to the ZX -basis of the qubits. In the data shown in Fig. 3, this means that the number of flips observed for the control qubit in Fig. 3A and for the target qubit in Fig. 3B are negligibly small, i.e., 0 error event and only 1 error event respectively over 943 total events. We can therefore describe the errors of the quantum gate in terms of dephasing between the ZX -eigenstates. In terms of the operator expansion of errors, we can define the correct operation \hat{U}_{gate} and three possible phase flip errors as

$$\begin{aligned} \hat{U}_{\text{gate}} &= |VV\rangle\langle VV| + |VH\rangle\langle VH| + |HV\rangle\langle HV| - |HH\rangle\langle HH|, \\ \hat{U}_T &= |VV\rangle\langle VV| - |VH\rangle\langle VH| + |HV\rangle\langle HV| + |HH\rangle\langle HH|, \\ \hat{U}_C &= |VV\rangle\langle VV| + |VH\rangle\langle VH| - |HV\rangle\langle HV| + |HH\rangle\langle HH|, \\ \hat{U}_{CT} &= |VV\rangle\langle VV| - |VH\rangle\langle VH| - |HV\rangle\langle HV| - |HH\rangle\langle HH|. \end{aligned} \quad [3]$$

The operation of the gate can then be written as

$$E(\rho_{\text{in}}) = \sum_{n,m} \chi_{nm} \hat{U}_n \rho_{\text{in}} \hat{U}_m, \quad [4]$$

where $n, m \in \{\text{gate}, T, C, CT\}$, and χ_{nm} define the process matrix of the noisy quantum process.

Each of our experimentally observed truth table operations $i \rightarrow j$ is correctly performed by \hat{U}_{gate} and one other operation \hat{U}_n . Therefore, the fidelities $F_{i \rightarrow j}$ can be given by the sums of the probability $F_p = \chi_{\text{gate, gate}}$ for the correct operation \hat{U}_{gate} and the probabilities $\eta_n = \chi_{nm}$ for the errors \hat{U}_n as follows.

$$\begin{aligned} F_{ZZ \rightarrow ZZ} &= F_p + \eta_T & F_{XX \rightarrow XX} &= F_p + \eta_C \\ F_{XZ \rightarrow YY} &= F_p + \eta_{CT}. \end{aligned} \quad [5]$$

Note that these relations between the diagonal elements of the process matrix and the experimentally observed fidelities can also be derived from Eq. 4 using the formal definition of the experimental fidelities. In this case the fidelities are determined by the sums over the correct outcomes $|j\rangle_l$ in $E(|i\rangle_k \langle i|_k)$, averaged over all inputs $|i\rangle_k$,

$$\begin{aligned} F_{i \rightarrow j} &= \sum_{l,k} \langle j\rangle_l E(|i\rangle_k \langle i|_k) \langle j\rangle_l / 4 \\ &= \sum_{n,m} \chi_{nm} \left(\sum_{l,k} \langle j\rangle_l \hat{U}_n^\dagger |i\rangle_k \langle i|_k \hat{U}_m |j\rangle_l / 4 \right). \end{aligned} \quad [6]$$

Here $k, l \in \{1, 2, 3, 4\}$, and $(i)_k$ denote the k th state of the i basis states. For example, $(i)_1 = |VV\rangle$, $(i)_2 = |VH\rangle$, $(i)_3 = |HV\rangle$, $(i)_4 = |HH\rangle$ for $i = ZX$. The sums over initial states k and final states l are one for $n = m = 0$ and for a single other error, $n = m = n(ij)$. All remaining sums are zero, confirming the results in Eq. 5.

Because the diagonal elements of the process matrix correspond to the probabilities of the orthogonal basis operations, their sum is normalized to one, so that $\sum_n \chi_{nm} = F_p + \eta_T + \eta_C + \eta_{CT} = 1$. It follows that the sum of all three experimentally determined fidelities is $F_{ZZ \rightarrow ZZ} + F_{XX \rightarrow XX} + F_{XZ \rightarrow YZ} = 2F_p + 1$. Therefore, the process fidelity of our KLM CNOT gate is given by

$$F_p = (F_{ZZ \rightarrow ZZ} + F_{XX \rightarrow XX} + F_{XZ \rightarrow YZ} - 1)/2 = 0.78. \quad [7]$$

This number clearly exceeds the threshold $F_p \geq 0.5$ for the gate to produce entanglement—a key quantum operation of the gate. The fidelity of the output states of the gate, averaged over all input states is related to the process fidelity

$$\bar{F} = (dF_p + 1)/(d + 1) = 0.82, \quad [8]$$

where d is the dimension of the Hilbert space ($d = 4$ for a two-qubit gate).

ACKNOWLEDGMENTS. We thank T. Nagata and M. Tanida for help and discussions. This work was supported in part by Quantum Cybernetics project, the Japan Science and Technology Agency (JST), Ministry of Internal Affairs and Communication (MIC), Japan Society for the Promotion of Science (JSPS), 21st Century Center of Excellence (COE) Program, Special Coordination Funds for Promoting Science and Technology, Daiwa Anglo-Japanese Foundation, European Research Council (ERC), Engineering and Physical Sciences Research Council (EPSRC), and Leverhulme Trust. J.L.O'B. acknowledges a Royal Society Wolfson Merit Award.

1. Ladd TD, et al. (2010) Quantum computers. *Nature* 464:45–53.
2. Gisin N, Thew R (2007) Quantum communication. *Nature Photonics* 1:165–171.
3. O'Brien JL, Furusawa A, Vučković J (2009) Photonic quantum technologies. *Nature Photonics* 3:687–695.
4. Giovannetti V, Lloyd S, Maccone L (2004) Quantum-enhanced measurements: beating the standard quantum limit. *Science* 306:1330–1336.
5. Nagata T, Okamoto R, O'Brien JL, Sasaki K, Takeuchi S (2007) Beating the standard quantum limit with four-entangled photons. *Science* 316:726–729.
6. Turchette QA, Hood CJ, Lange W, Mabuchi H, Kimble HJ (1995) Measurement of conditional phase shifts for quantum logic. *Phys Rev Lett* 75:4710–4713.
7. Schmidt H, Imamoglu A (1996) Giant Kerr nonlinearities obtained by electromagnetically induced transparency. *Opt Lett* 21:1936–1938.
8. Takeuchi S (1996) A simple quantum computer: experimental realization of the Deutsch Jozsa algorithm with linear optics. *Proceedings of Fourth Workshop on Physics and Computation* (New England Complex Systems Institute, Cambridge, MA), pp 299–302.
9. Takeuchi S (2001) Experimental demonstration of a three-qubit quantum computation algorithm using a single photon and linear optics. *Phys Rev A* 62:032301.
10. Cerf NJ, Adami C, Kwiat PG (1998) Optical simulation of quantum logic. *Phys Rev A* 57: R1477–R1480.
11. Knill E, Laflamme R, Milburn GJ (2001) A scheme for efficient quantum computation with linear optics. *Nature* 409:46–52.
12. Shields AJ (2007) Semiconductor quantum light sources. *Nature Photonics* 1:215–223.
13. Kim J, Takeuchi S, Yamamoto Y, Hogue HH (1999) Multiphoton detection using visible light photon counter. *Appl Phys Lett* 74:902–904.
14. Gottesman D, Chuang IL (1999) Demonstrating the viability of universal quantum computation using teleportation and single-qubit operations. *Nature* 402:390–393.
15. Gao WB, et al. (2010) Teleportation-based realization of an optical quantum two-qubit entangling gate. *Proc Natl Acad Sci USA* 107:20869–20874.
16. Bennett CH, et al. (1993) Teleporting an unknown quantum state via dual classical and Einstein-Podolsky-Rosen channels. *Phys Rev Lett* 70:1895–1899.
17. Bouwmeester D, et al. (1997) Experimental quantum teleportation. *Nature* 390:575–579.
18. Kok P, et al. (2007) Linear optical quantum computing with photonic qubits. *Rev Mod Phys* 79:135–174.
19. Pittman TB, Fitch MJ, Jacobs BC, Franson JD (2003) Experimental controlled-not logic gate for single photons in the coincidence basis. *Phys Rev A* 68:032316.
20. O'Brien JL, Pryde GJ, White AG, Ralph TC, Branning D (2003) Demonstration of an all-optical quantum controlled-NOT gate. *Nature* 426:264–267.
21. Sanaka K, Jennewein T, Pan JW, Resch K, Zeilinger A (2004) Experimental nonlinear sign shift for linear optics quantum computation. *Phys Rev Lett* 92:017902.
22. Gasparoni S, Pan JW, Walther P, Rudolph T, Zeilinger A (2004) Realization of a photonic controlled-NOT gate sufficient for quantum computation. *Phys Rev Lett* 93:020504.
23. Zhao Z, et al. (2005) Experimental demonstration of a nondestructive controlled-NOT quantum gate for two independent photon qubits. *Phys Rev Lett* 94:030501.
24. Okamoto R, Hofmann HF, Takeuchi S, Sasaki K (2005) Demonstration of an optical quantum controlled-not gate without path interference. *Phys Rev Lett* 95:210506.
25. Langford NK, et al. (2005) Demonstration of a simple entangling optical gate and its use in bell-state analysis. *Phys Rev Lett* 95:210504.
26. Kiesel N, Schmid C, Weber U, Ursin R, Weinfurter H (2005) Linear optics controlled-phase gate made simple. *Phys Rev Lett* 95:210505.
27. Bao XH, et al. (2007) Optical nondestructive controlled-not gate without using entangled photons. *Phys Rev Lett* 98:170502.
28. Politi A, Cryan MJ, Rarity JG, Yu S, O'Brien JL (2008) Silica-on-silicon waveguide quantum circuits. *Science* 320:646–649.
29. Okamoto R, et al. (2009) An entanglement filter. *Science* 323:483–485.
30. Gao WB, et al. (2011) Experimental measurement-based quantum computing beyond the cluster-state model. *Nature Photonics* 5:117–123.
31. Lanyon BP, et al. (2010) Towards quantum chemistry on a quantum computer. *Nature Chemistry* 2:106–111.
32. Saunders DJ, et al. (2010) Experimental EPR-steering using Bell-local states. *Nat Phys* 6:845–849.
33. Schmid C, et al. (2009) Quantum teleportation and entanglement swapping with linear optics logic gates. *New J Phys* 11:033008.
34. Hong CK, Ou ZY, Mandel L (1987) Measurement of subpicosecond time intervals between two photons by interference. *Phys Rev Lett* 59:2044–2046.
35. Ralph TC, White AG, Munro WJ, Milburn GJ (2001) Simple scheme for efficient linear optics quantum gates. *Phys Rev A* 65:012314.
36. Horodecki M, Horodecki P, Horodecki R (1999) General teleportation channel, singlet fraction, and quasidistillation. *Phys Rev A* 60:1888–1898.
37. Gilchrist A, Langford NK, Nielsen MA (2005) Distance measures to compare real and ideal quantum processes. *Phys Rev A* 71:062310.
38. Nielsen MA (2004) Optical quantum computation using cluster states. *Phys Rev Lett* 93:040503.
39. Kok P (2002) Single-photon quantum-nondemolition detectors constructed with linear optics and projective measurements. *Phys Rev A* 66:063814.
40. Resch KJ (2004) Spatiotemporal few-photon optical nonlinearities through linear optics and measurement. *Phys Rev A* 70:051803(R).
41. Fushman I, et al. (2008) Controlled phase shifts with a single quantum dot. *Science* 320:769–772.
42. Aoki T, et al. (2009) Efficient routing of single photons by one atom and a microtoroidal cavity. *Phys Rev Lett* 102:083601.
43. Matsuda N, Shimizu R, Mitsumori Y, Kosaka H, Edamatsu K (2009) Observation of optical-fibre Kerr nonlinearity at the single-photon level. *Nature Photonics* 3:95–98.